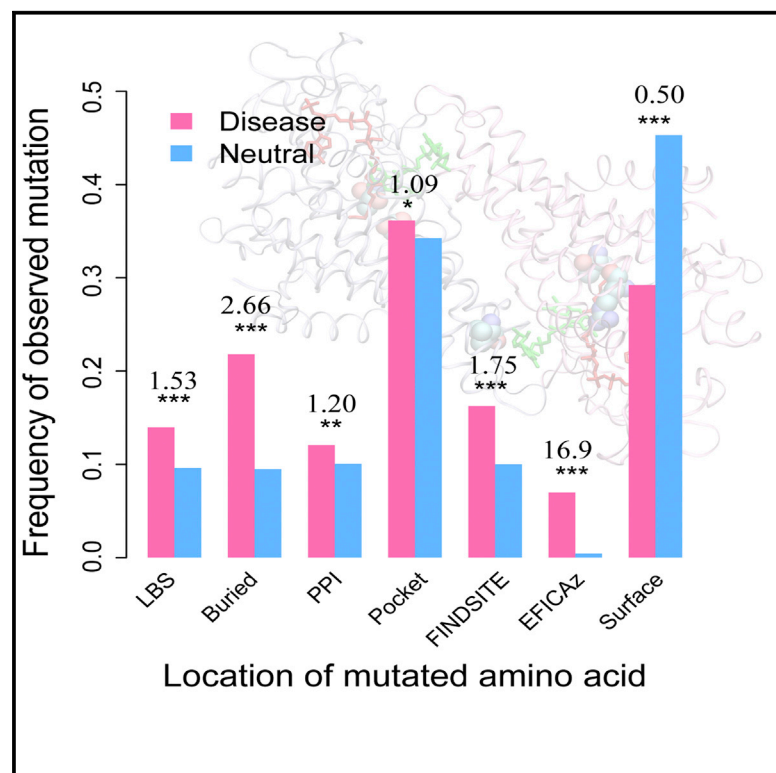


Structure

Insights into Disease-Associated Mutations in the Human Proteome through Protein Structural Analysis

Graphical Abstract



Authors

Mu Gao, Hongyi Zhou, Jeffrey Skolnick

Correspondence

skolnick@gatech.edu

In Brief

Atomic structures and functional analysis of proteins can provide invaluable insights into why certain variations are disease associated. Using experimental structural data and computational predictions of functional effects, Gao et al. provide a comprehensive analysis and structural rationalization of thousands of disease-associated and neutral variations.

Highlights

- A comparative structural analysis of disease-associated and neutral mutations
- Assessment of structural regions most vulnerable to disease mutations
- Variations adjacent to protein-protein interfaces are strongly disease associated
- Compositional analysis in comparison with mutations from the 1K Genomes Project



Insights into Disease-Associated Mutations in the Human Proteome through Protein Structural Analysis

Mu Gao,¹ Hongyi Zhou,¹ and Jeffrey Skolnick^{1,*}

¹Center for the Study of Systems Biology, School of Biology, Georgia Institute of Technology, 250 14th Street NW, Atlanta, GA 30318, USA

*Correspondence: skolnick@gatech.edu

<http://dx.doi.org/10.1016/j.str.2015.03.028>

SUMMARY

Most known disease-associated mutations are missense mutations involving changes of amino acids of proteins encoded by their genes. Given the plethora of genetic studies, sequenced exomes, and new protein structures determined each year, it is appropriate to revisit the role that structure plays in providing insights into the molecular basis of disease-associated mutations. In that regard, a large-scale structural analysis of 6,025 disease-associated mutations as well as 4,536 neutral variations for comparison was performed. While buried amino acids are common among the disease-associated mutations, as reported previously, more are statistically significantly enriched at observed or predicted functional sites. Interesting findings are that ligand-binding sites adjacent to protein-protein interfaces and residues involved in enzymatic function are especially vulnerable to disease-associated mutations. Finally, a compositional analysis of disease-associated mutations in comparison with variants identified in the 1000 Genomes Project provides a structural rationalization of the most disease-associated residue types.

INTRODUCTION

Since the sequencing of the first human genome was completed a decade ago (Collins et al., 2004), tremendous efforts have been made to advance new sequencing methods that allow rapid, massively parallel sequencing at low cost (Metzker, 2010). These next-generation sequencing methods enable large-scale sequencing on thousands of individuals, generating a large amount of data available for comparative genome analysis (Abecasis et al., 2010, 2012). By identifying variations of DNA sequences, in particular, Single Nucleotide Polymorphisms (SNPs), we may begin to decipher the links between phenotypes and genotypes. Of particular interest are genetic mutations that cause various human, especially Mendelian, diseases. Statistical analyses of patients' and normal people's sequences often pinpoint mutations strongly associated with patients. Many such mutations are collected in databases such as the Online Database of Mendelian

Inheritance in Man (OMIM) (McKusick, 2007) and the Human Gene Mutation Database (HGMD) (Stenson et al., 2008).

Since most cases in these databases are SNPs identified through statistical analysis, it is not clear whether a particular mutation is actually the cause of the implicated disease. These mutations are usually referred to as being disease associated. Most are non-synonymous SNPs (nsSNPs), which occur in the coding regions of genes and result in changes of amino acid type, i.e., missense mutations. It is therefore expected that the change of amino acid impairs the function of the involved protein. However, for the vast majority of cases, it is not clear how the mutation affects the function of the protein. In this regard, studying the impact of mutations may provide a better understanding of the mechanisms of the corresponding diseases and eventually may significantly increase the chance of finding a better treatment for patients with the disease.

Meanwhile, over a comparable period, the three-dimensional structures of many proteins have been determined at high resolution (Berman et al., 2000). Often, these proteins are co-crystallized with other biomolecules that are relevant to their functions, e.g., protein-protein complexes and protein-ligand complexes. Given these structural data, many questions regarding disease-causing mutations can be asked and addressed by a thorough inspection of these structures: can we understand disease-associated mutations in the context of their locations in the structure of the protein? Where are disease-linked missense mutations located in the proteins? What are the functional and structural consequences of these mutations? Is there any location in the protein where variations are more likely to cause disease? What is the structural reason why certain types of mutations are more likely to be disease associated? Answers to these questions not only deepen our understanding of the molecular mechanisms of diseases but also have practical implications for the predictions of disease association by automated computational tools and for personalized medicine.

Over a decade ago, Wang and Moult (2001) performed an early study of 262 disease-associated mutations from 26 proteins and found that about 80% of them destabilize proteins and about 5% involve ligand binding. A subsequent study by Steward et al. (2003) of 1,292 mutations from 63 proteins showed that about 28% are buried and related to protein stability, while 29% are involved in intermolecular interactions such as protein-protein interactions and ligand binding. Similar results were also reported in another study (Sunyaev et al., 2000). However, mainly due to the paucity of solved protein structures, these studies were carried out on very few proteins. Since then, many new

Table 1. Locations of Disease-Associated Amino Acid Mutations in Protein Structures

Location	Count (Frequency)
Buried	2,211 (0.22)
PPI	726 (0.12)
Ligand binding	714 (0.12)
Metal ion binding	174 (0.029)
DNA/RNA binding	42 (0.007)
Geometric pocket	2,177 (0.36)
EFICAz	420 (0.07)
FINDSITE	738 (0.12)
Other (exposed)	1,451 (0.30)
Total	6,025

disease-causing mutations have been found, and the number of known protein structures has also grown exponentially, especially for those in complex with functional partners. The previous studies also lacked a comparison with neutral variations. The statistical significance of their discoveries, in particular, the value of structural analysis to the prediction of disease association, is unclear.

Given this background, it is worthwhile revisiting the questions raised above. In this study, we performed a large-scale analysis of 6,025 disease-associated mutations in 642 proteins with experimental structures, as well as 4,536 neutral mutations in 1,743 proteins for comparison. We took advantage of the fact that many of these proteins have multiple structures in complex with other proteins or ligands. Below, we first map these mutations to their locations onto protein structures. We then compare them with neutral variations and identify regions more likely to cause disease. We also analyze the likelihood that different amino acid types are disease associated and provide structural explanations for some of the most deleterious mutations.

RESULTS

We have collected 6,025 disease-associated missense mutations in 642 human genes and 4,536 neutral mutations in 1,743 human genes from the August, 2013 release of the UniProt (Universal Protein Resource) database (see [Experimental Procedures](#)) (Wu et al., 2006). All these mutations have at least one experimentally determined protein structure containing the corresponding mutation. The locations of these mutations are subsequently analyzed.

Where Are the Disease-Associated Missense Mutations in Their Protein Structures?

Table 1 shows the statistics of disease-associated mutations. About 22% are buried in protein cores; 12% are found at protein-protein interfaces (PPIs); 36% are located in concave pockets; 12% and 2.9% are found in direct physical contact with small-molecule ligands and metal ions, respectively; and a small fraction, 0.7%, are at either DNA-protein or RNA-protein interfaces. Since the experimental information is most likely incomplete, we further applied two computational tools, EFICAz for enzyme function prediction (Kumar and Skolnick, 2012) and

FINDSITE^{comb} for ligand-binding site predictions, to our datasets (Zhou and Skolnick, 2013). About 7% of disease-associated mutations are classified by EFICAz as being functional discriminating residues (FDRs) for their corresponding enzymatic functions, and an additional 12% of mutations are at FINDSITE^{comb} predicted ligand-binding sites that did not have bound ligands in their PDB structures. It should be noted that these location classifications are not necessarily mutually exclusive, e.g., about 69% and 45% of observed small-molecule ligand-binding sites are found in geometric pockets or predicted by FINDSITE^{comb}, respectively. Another interesting observation is that about 15% of disease-associated mutations of observed ligand-binding sites are also identified at the PPIs. This is investigated in detail below.

Figure 1 shows a pie chart obtained by assigning a unique primary location to each mutation, using the following order: DNA/RNA binding, ion binding, small-molecule ligand binding, PPI, buried, EFICAz, FINDSITE^{comb}, pocket, and other exposed. About 15% of disease-associated mutations are located at known functional sites, i.e., they involve binding to other molecules than proteins; 10% are at PPIs; and 20% of mutations are within protein cores and are likely important for maintaining stability. EFICAz and FINDSITE^{comb} in addition flagged 3% and 5% of mutations that are potentially important for the functions of the corresponding protein. After these classifications, 17% of mutations are found in pockets, which might engage in unknown interactions with some biomolecules. Overall, this classification scheme could assign a primary functional or structural role for 70% of disease-associated mutations. The remaining 30% of mutations involve exposed surface residues and are located at either a flat surface or small pocket. They are potentially candidate interaction sites for unknown protein-protein interactions or interactions with biomolecules that do not require large concave pockets.

How Useful Is Structural/Functional Information for Predicting Disease Association?

In order to answer this question, we compared the frequency of disease-associated mutations versus neutral mutations at different locations derived from our structural and functional analysis mentioned above. As shown in Figure 2A, in all locations except for unannotated, exposed regions, disease mutations are more likely to appear than neutral mutations. In the protein interior, the frequency of disease mutations is over two times that of neutral mutations. This gives an odds ratio (OR) of 2.66, which is the odds of disease versus neutral among buried mutations over the odds of disease versus neutral among all other mutations in our sets. The result is statistically highly significant, with a p value 4.0×10^{-67} (Fisher's exact test, two-tailed). Likewise, ligand-binding sites are about 50% more likely to be observed in the disease set than in the neutral set, which gives a significant OR of 1.53 ($p = 6.8 \times 10^{-12}$). At an OR of 1.75 ($p = 4.4 \times 10^{-21}$), the performance of FINDSITE^{comb} in terms of OR is slightly better than that obtained by counting observed ligand-binding sites in experimental structures. Within a PPI, or pocket region, disease mutations are slightly, but significantly, more frequent than neutral mutations, yielding ORs of 1.23 ($p = 1.3 \times 10^{-3}$) and 1.09 ($p = 0.04$), respectively. The latter is less significant, partly due to the fact that not all

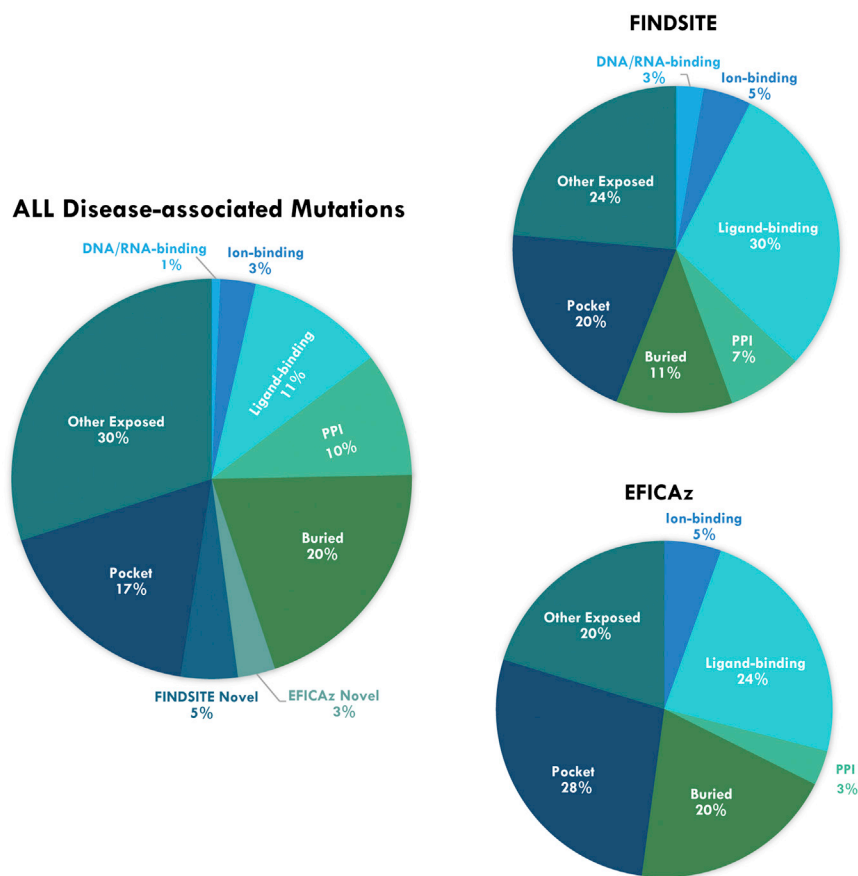


Figure 1. Pie Charts of Disease-Associated Mutations According to Their Primary Locations

On the left are the overall distributions; on the right are the charts of positive hits by FINDSITE and EFICAZ, respectively.

expected, as surface residues without a functional or structural role are less likely to cause disease.

Since neutral mutations are from a much more diverse set of proteins than disease-associated mutations (1,743 versus 642 proteins), there is the concern that the dataset might be biased. In order to eliminate such a concern, we further performed the same analysis on the subset of mutations that appear in the same set of proteins. Figure 2B shows results that qualitatively are in agreement with the analysis on the full set shown above.

Mutations Adjacent to PPIs Are More Likely Associated with Disease Than Mutations within PPIs

Overall, about 58% of disease-associated mutations are found in at least one protein-protein complex structure versus 50% of neutral mutations that are found in a protein-protein complex. We further analyzed the distribution of mutations in

residues identified in a predicted, geometric protein pocket are important for protein function or stability; thus, there are more noisy signals in this region. Surprisingly, EFICAZ predictions have the highest OR, of about 17 ($p = 1.6 \times 10^{-78}$). Many of these predictions are at highly conserved active sites important for enzymatic function, although they cover only about 7% of disease mutations. On the other hand, among unannotated surface residues, neutral mutations have a high percentage at 45%, compared with about 30% of disease mutations. This is

protein-protein complexes according to their distance from observed PPIs (Figure 3A). As shown above, about 12.0% of all disease mutations and 10.1% of neutral mutations in our datasets are located at the PPIs, i.e., 0 Å from the interface. This gives a small, but statistically significant, difference of 1.9%, corresponding to an increase of about 20% in OR to 1.23 for the disease-associated mutations. The remaining difference in cumulative fraction comes mainly from the mutations close to but not at the PPIs. Within 3 Å from PPIs, the cumulative difference

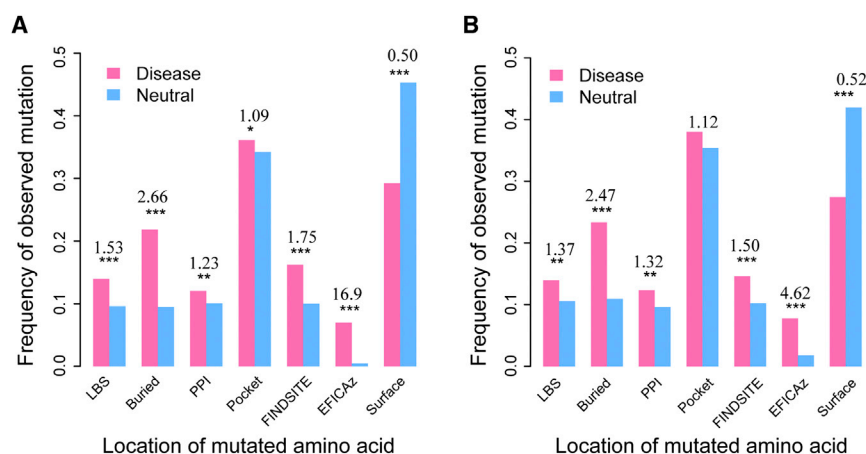


Figure 2. Disease-Associated Mutations Versus Neutral Ones Assigned by Their Location in the Structure of the Protein

Each bar represents the fraction of mutations in either disease-associated or neutral datasets. The numbers above pairs of bars are the ORs. Asterisks denote statistical significance according to one-tailed Fisher's exact test (*0.01 < P < 0.05; **0.001 < P < 0.01; ***P < 0.001; no asterisk, P > 0.05).

(A) All mutations.
(B) Subset of mutations from the same set of proteins that contain both disease-associated and neutral mutations.
LBS, ligand-binding sites.

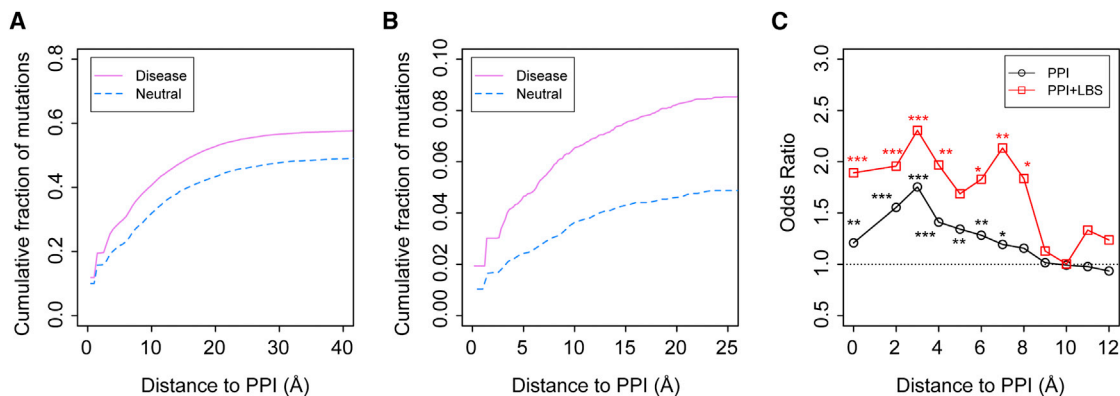


Figure 3. Distribution of Mutations in the Neighborhood of PPIs

(A) Cumulative fractions of disease-associated mutations versus neutral ones according to their distance from known PPIs.

(B) Subsets of mutations that are also observed at small-molecule ligand-binding sites (LBS).

(C) Distributions of ORs according to distance from PPIs. A bin width of 2 Å is employed. Asterisks represent statistical significance as in Figure 2.

rapidly increases to 6.8%; this percentage further increases to 8.3% within 6 Å from PPIs. Thus, it appears that disease mutations are more likely to occur at and/or adjacent to PPIs than neutral mutations. Moreover, the biggest difference is attributed to regions immediately neighboring PPIs, i.e., at a distance from 0 Å to 6 Å, rather than at the PPIs themselves. This difference leads to a significant increase of OR values to as high as 1.75 at 3 Å from PPIs (Figure 3C).

Since disease-causing mutations are more likely to be buried than neutral mutations, as shown in Figure 2, one natural explanation is that buried mutations close to PPIs are more likely disease associated than neutral. The difference in cumulative fraction of buried mutations around PPIs between the disease and neutral sets is about 0.1% at 0 Å, 3.5% within 3 Å, and 5.1% within 6 Å from PPIs. Therefore, mutations of buried residues do make a major contribution to the observed phenomenon. However, this explains only about 61% of the observed difference.

A second main reason for this phenomenon is that adjacent to PPIs, there are functionally relevant pockets involving ligand recognition. It has been shown that protein-protein association naturally creates geometric pockets (Gao and Skolnick, 2012). Some of these pockets could be selected by evolution for ligand binding. As a result, functionally relevant ligand-binding pockets are enriched around PPIs. Mutations at these pockets likely lead to harmful effects. Indeed, if we focus on the subset of mutations that are also ligand binding within protein-protein complexes, we find that disease-associated mutations are much more likely to be found in the neighborhood of PPIs versus neutral mutations. As shown in Figure 3B, the difference in the cumulative fraction of mutations is 0.9% at 0 Å from PPIs, 2.0% within 3 Å from PPIs, and 2.6% within 6 Å, which could explain about 31% of the corresponding 8.3% difference in overall cumulative fraction difference mentioned above. This also contributes to an overall bump in the OR shown in Figure 3C. Notice that the risk of being disease associated is about 30% higher in terms of OR when a mutation is observed in a ligand-binding site within 3 Å from a PPI.

Figure 4 shows two examples of disease-associated mutations located at/near PPIs. Medium-chain acyl-coenzyme A

(CoA) dehydrogenase (ACADM) is one of four enzymes involved in fatty acid catabolism (Lee et al., 1996). The enzyme is responsible for the α,β -dehydrogenation of fatty acyl-CoA derivatives. The structure of this protein is a dimer of dimers. Figure 4A shows the structure of the basic dimer unit, in which the co-factor FAD (flavin-adenine dinucleotide) is sitting at the dimeric interface, whereas the fatty substrate is located close by. There are five known mutations located in the binding sites of these substrates within 5 Å. They are linked to ACADM (ACADM medium-chain deficiency), a disease that can cause sudden death of infants (OMIM: 201450).

One important benefit of an interfacial pocket formed adjacent to PPIs is that it could function as a molecular switch controlled by the association/dissociation of the protein complex. This is illustrated in an example involving two proteins, retinitis pigmentosa 2 (RP2) and the small G protein Arf-like 3 (Arl3), which form a complex providing a guanosine triphosphate binding pocket at the PPI (Figure 4B) (Veltel et al., 2008). It is thought that this is a molecular switch for regulating the ciliary process in photoreceptor cells. Mutations in RP2 that disrupt ligand binding at the PPI, such as the arginine finger R118, may cause X chromosome-linked eye disease (OMIM: 312600).

Post-Translational Modifications and Disease Association

Post-translational modifications play essential roles in many biological processes. We examined how many disease-associated mutations are located at such a site compared with neutral mutations. From the UniProt knowledge base, we searched for experimentally validated modification sites. We found only 27 cases in the disease mutation set and 11 cases in the neutral set, which gives a p value of 0.1 (Fisher's exact test, two-tailed). The most common modifications are glycosylation: nine in the disease mutations and four in the neutral mutations. If we drop the requirement of having solved structures, we are able to match 77 of 23,846 disease mutations and 68 of 37,687 neutral mutations, which leads to a significant p value of 5.9×10^{-4} . As one would expect, mutations at post-translational

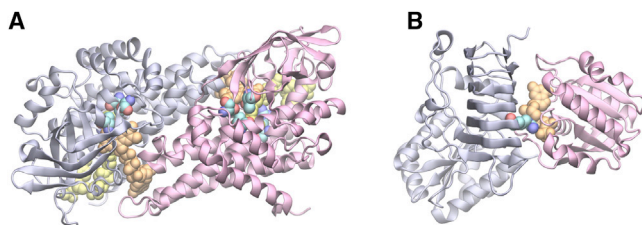


Figure 4. Examples of Disease-Associated Mutations Observed in the Neighborhood of PPIs

(A) Dimeric ACADM.

(B) Retinitis pigmentosa 2 and Arl3. In each snapshot, protein structures are shown in light blue and purple cartoon representations, small molecules are shown in orange and yellow van der Waals (VdW) representations, and reference amino acids at the mutation sites are also shown in VdW representations, where carbon, oxygen, and nitrogen atoms are colored in cyan, red, and blue, respectively.

modification sites are significantly more likely to be associated with disease. However, the cases that can be explained by such mutations are very small, to the best of our knowledge.

Amino Acid Changes and Disease Association

Finally, we ask the question whether there are certain types of amino acid changes that are more likely to be disease associated. Figure 5A shows the frequency of amino acid types from the original reference amino acid at the mutation sites. Arginine is the most common mutation in both disease and neutral sets, due to the fact that four of the six arginine codons contain the CpG dinucleotide, which is relatively vulnerable to mutations (Cooper and Youssoufian, 1988). However, because the frequencies of arginine mutations in these two sets are very close, 14.8% versus 14.3%, it is not a good indicator for predicting disease association. In terms of OR, mutation from Cys is highest at 4.86, followed by Trp at 3.58, and glycine at 2.04. On the other hand, mutations involving certain hydrophobic residues, such as valine and isoleucine, are significantly underrepresented in disease mutations. One explanation is that valine and isoleucine have similar physicochemical properties and are very close in the codon space, with only a single nucleotide difference (GUA, GUC, GUU of valine and AUA, AUC, AUU of isoleucine).

Figure 5B shows the frequencies of amino acids to different mutated residues. Statistical analysis suggests that mutation to Pro is most likely damaging, with an OR of 3.46, followed by CYS at 1.87. It is interesting to note that the frequencies of disease-causing mutations show a much lower correlation to frequencies of neutral mutations when one compares mutated-to amino acids versus mutation-from amino acids. The corresponding Pearson correlation coefficients are 0.35 versus 0.73. This suggests that the mutation-from frequencies are largely determined by similar reasons, for example, distribution of codons and distances in the codon space (i.e., those with one nucleotide difference are of high possibilities), whereas mutation-to frequencies are largely determined by very different reasons between the disease and neutral sets.

The 1000 Genomes Project has revealed a large set of variants in about 1,000 healthy individuals (Abecasis et al., 2012). One could argue that these variants are a good neutral background for the purpose of our analysis. We repeated the same composi-

tion analysis using the data from the 1000 Genomes Project. As shown in Figures 5C and 5D, we obtained very similar results to those using the UniProt neutral set. Mutations from and to CYS give an OR of 2.79 and 1.33, respectively; mutations from Trp have an OR of 3.58; and the OR of mutations to Pro is 3.21. These are also mutations that are most likely associated with diseases than neutral mutations.

We then sought structural explanation for the top three most deleterious types of mutations involving Cys, Pro, and Trp amino acids. First, we ask why mutations from and to a Cys residue are harmful. Since it is known that Cys often form disulfide bonds, it is hypothesized that a Cys mutation either disrupts useful disulfide bonds in the case of mutation from or introduces an unwanted disulfide bond in case of mutation to. To test this hypothesis, we examined if there are Cys disulfide bonds in the structure of the corresponding protein. In the mutation-from set, about 2/3 of Cys mutations are likely to form a disulfide bond with another Cys residue nearby within 4.5 Å, whereas only about 1/3 of Cys mutations in the neutral set have another Cys nearby. This gives a highly significant p value of 3.2×10^{-6} . Therefore, disease-associated Cys mutations are more likely to disrupt an original disulfide bond important for protein stability or function. On the other hand, in the mutation-to datasets, we found that after the mutation to Cys, there are 45 cases in which there is another Cys nearby in the disease set, versus only seven cases in the neutral set ($p = 0.007$). In these cases, the Cys mutation may introduce an unwanted disulfide bond that could lead to protein malfunction.

Second, why is a mutation to Pro likely to be harmful? Pro is a unique amino acid that does not have an hydrogen for backbone hydrogen bond formation. In addition, it has a more restricted dihedral angle space than a typical amino acid. This restriction often creates a kink in helical structures at the position of a Pro. As a result, mutations to Pro often disrupt helical structures. We performed an analysis of the secondary structure where a mutation to Pro occurs, with the result shown in Table 2. The most common Pro mutation in the disease set lies within a 3_{10} helix, about 36%, in contrast to 23% cases in the neutral set ($p = 0.006$). The second common secondary structural element where a Pro mutation occurs is a turn: 26% in disease versus 18% in neutral ($p = 0.1$) sites, where a Pro mutation might disrupt hydrogen bonding. By contrast, in the coil region, where there is no ordered secondary structure, a Pro mutation is much less likely present at 20%, in comparison with 32% in the neutral set ($p = 0.009$). The result supports the conclusion that the disruptive presence of a Pro mutation in the secondary structure is often disease associated.

Lastly, we investigated mutation from Trp that is often linked to disease. Trp is the largest amino acid that plays an important role in protein folding and stability. On average, a Trp residue makes 8.5 side-chain contacts versus 6.0 side-chain contacts of other types of amino acids. Further calculation estimates that a Trp mutation in the disease set leads to a mean increase of the free energy of protein folding $\Delta\Delta G$ of 3.4 kcal/mol (126 cases, SD = 1.61 kcal/mol), versus 2.9 kcal/mol (27 cases, SD = 1.36 kcal/mol) of Trp mutations in the neutral set ($p = 0.076$, t test, two-tailed). This analysis suggests that mutations from Trp likely destabilize the structure of the protein and result in less fitness. In the vast majority of cases analyzed, this

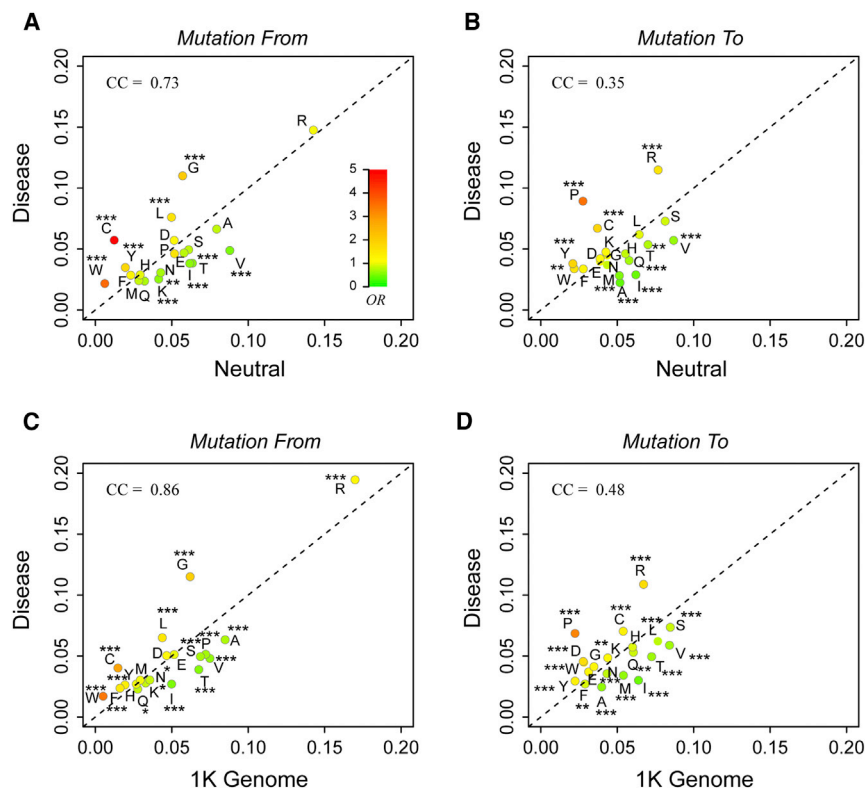


Figure 5. Composition Analysis of Disease-Associated Mutations Versus Neutral Mutations from the UniProt database and the 1000 Genomes Database

Amino acids are labeled by their one-letter names. The color of each type of amino acid represents ORs of disease mutations versus neutral ones. The same color scale of OR shown as the insert in (A) is adopted throughout all other panels. Statistical significance of association is indicated by asterisks in the same way as in Figure 2. CC, Pearson correlation coefficient. The dashed line represents an OR of 1. (A and B), from the UniProt database; (C and D), from the 1000 Genomes Database

destabilization likely has a significant impact on the function of protein, thus leading to various disease conditions.

DISCUSSION

Since the vast majority of disease-associated mutations are assigned based on statistical analysis, it is not clear whether a mutation is actually the cause of the implicated disease. To provide a better understanding of mutations from a structural perspective, we performed a large-scale analysis of 6,025 disease-associated mutations in 642 proteins. We found that about 20% of mutations are buried in protein cores and that these mutations may destabilize protein structures, whereas about 11% of mutations are involved in ligand binding, and another 10% are involved in protein-protein interactions. About 17% are in pockets, 3% involve ion binding, and 1% DNA/RNA binding. These numbers are consistent with previous studies conducted on smaller datasets (Steward et al., 2003; Sunyaev et al., 2000). Using computational approaches, we further predicted that about another 8% of mutations are likely ligand-binding or essential for enzyme function. We found a structural/functional annotation for about 70% of mutations. As more experimental structures are determined for functional complexes of proteins, e.g., in complex with other ligand or proteins for their function, we expect to see more mutations explained by the functional roles of the mutated residues.

In order to demonstrate the usefulness of the structural/functional data, one needs to compare disease-associated mutations with neutral mutations. This has been largely

ignored or not thoroughly pursued in previous studies. Here, we show a statistically significant difference between disease-associated and neutral mutations. As pointed out previously (Ng and Henikoff, 2006), one of the most effective descriptors is the degree of surface exposure of the protein residue at the mutation site. Buried residues in the disease set have the second highest OR, at 2.66, compared with neutral ones, whereas exposed residues not involving any interactions or pocket-like feature are more likely to be neutral at an OR of 0.50. Functional sites, such as ligand-binding sites and PPI residues, all have significant ORs at 1.53 and 1.23. However, they are not as effective as one naively expects. One reason might be due to purification selections, which removed many deleterious, fatal mutations at these functional sites. It is also worth mentioning that computational predictions achieved good performance. Predictions by FINDSITE^{comb} and EFICAZ yield OR values at 1.75 and 16.9, respectively, which is comparable with or better than results obtained by counting known ligand-binding sites from experimental structures. Most interestingly, it is the predicted loss of enzymatic function that is most strongly disease associated. These are encouraging results, which demonstrate the potential of computational, knowledge-based methods.

One novel observation is that mutations adjacent to PPIs are more likely associated with disease than mutations at the PPIs themselves. At 1.75, the OR is highest about 3 Å from PPIs, which is about 40% higher than the OR at PPIs. There are two contributing factors. One is that the mutations at buried sites within each monomer but close to the PPIs are more likely to be disease causing, presumably by destabilizing the protein complex. The second is due to the presence of interfacial pockets, which are ligand-binding pockets at or adjacent to PPIs (Gao and Skolnick, 2012). Mutations within interfacial pockets could disrupt functionally important ligand-protein interactions. This is supported by subsequent analysis, which shows that mutations within interfacial pockets have more than double the OR of mutations at PPIs.

Although amino acid type change is one main factor for assessing pathogenicity of human mutations in many automatic

Table 2. Analysis of Secondary Structure Location of Mutations to Proline

Type	Disease	Neutral	P^a
3_{10} helix	195 (0.36)	29 (0.23)	0.003
α helix	21 (0.039)	7 (0.056)	–
Turn	139 (0.26)	23 (0.18)	0.049
β sheet	38 (0.071)	11 (0.088)	–
Bend	35 (0.065)	15 (0.12)	–
Coil	110 (0.20)	40 (0.32)	0.005
Total	538	125	

^aInsignificant P value is indicated by –.

annotation tools (Adzhubei et al., 2010; Kumar et al., 2009), in-depth analysis of why it works is somewhat lacking, although there have been studies about the frequencies of disease-associated mutations (de Beer et al., 2013; Vitkup et al., 2003). Obviously, if the mutation involves very different amino acid types, e.g., from hydrophobic to charged residues, it is more likely to cause an issue than mutations among hydrophobic residues. Ideally, one would like to study all 380 pairs of non-synonymous mutations. However, the number of known disease-causing mutations is currently too limited for such a study. We opt instead to focus on each type of amino acid, grouped by mutations from and mutation to a given amino acid type. We found that certain types of mutations, such as mutations involving Cys, Trp, or Pro, are more likely to be disease associated. Through structural analysis, Cys mutations often involve breaking disulfide bridges or forming unwanted disulfide bonds; Trp mutations usually significantly destabilize structures, and mutations to Pro tend to disrupt helical structures. These analyses provide some examples of how structural analysis could provide further insights into the mechanisms of disease.

EXPERIMENTAL PROCEDURES

Dataset

From the August, 2013 release of the UniProt knowledge base (Wu et al., 2006), we collected 23,846 disease-associated variants and 37,782 polymorphisms in human; we assume that the latter are neutral mutations. The classification was manually assigned according to the literature and a previously curated database such as OMIM (McKusick, 2007). These variants are all missense mutations with changes of amino acid type. Unclassified variants were ignored. From this collection, we further selected those with at least one experimentally determined structure deposited in the PDB (Berman et al., 2000). We verified that the protein structure contains the same amino acid at the position indicated in the UniProt mutation data. To avoid possible bias, if the gene contains more than 50 variants, we randomly selected no more than 50 variants in each gene. If multiple variants are found corresponding to the same residue position in a gene, we also randomly selected only one variant. This procedure yielded 6,025 disease-associated mutations in 642 proteins and 4,536 neutral mutations in 1,743 proteins. These two sets are the main dataset used in our study. They share 355 common proteins, with 4,209 disease mutations and 1,113 neutral mutations.

Data of the 1000 Genomes Project variants are from de Beer et al. (2013). It should be noted that the counts of mutations from OMIM are mislabeled in that study. The counts of mutations from were mistaken as mutation to, and vice versa. The mistake in de Beer et al. (2013) gives incorrect amino acid mutation frequencies, which are inconsistent with a previous study (Vitkup et al., 2003), whereas our results are in agreement with Vitkup et al. (2003).

Table 3. Contingency Table for the Statistical Test

	Disease	Neutral	Odds
Positive	d_{pos}	n_{pos}	d_{pos}/n_{pos}
Negative	d_{neg}	n_{neg}	d_{neg}/n_{neg}
Total	6,025	4,325	–

Structural and Functional Analysis

Using the experimental structures, we mapped the location of each mutation. For each PDB record, we analyzed the structure given by the basic asymmetric unit, as well as author assigned biounit if it contains protein-protein complexes. The HET code in each PDB header was used to determine the types of ligand, i.e., metal ion, small-molecule ligand, or DNA/RNA. Note that this analysis does not guarantee that a ligand has biologically relevant interaction with its co-crystallized protein. Nevertheless, in many cases, biologically relevant molecules recognize the same binding sites on proteins as other non-biological molecules. Atomic contacts between protein and ligand were determined by the program LPC (Sobolev et al., 1999). If the original amino acid at the mutation site contains at least one heavy atom making physical contact with a ligand, it is assigned as ligand binding. Similarly, PPI residues are defined by a heavy-atom distance of 4.5 Å. The distance between a variant residue and PPI is defined as the shortest heavy-atom distance between the residue and any PPI residue. If a protein has multiple complex structures, we chose the minimal distance among all these complexes. Solvent accessible surface area (SASA) was calculated for each original residue of the mutations using the program NACCESS (Hubbard and Thornton, 1993). If a residue has less than a 1% relative SASA percentage, it is defined as a buried residue. Otherwise, the residue is an exposed surface residue. Again, if the residue is observed in multiple structures, we employed the lowest relative SASA value. We also ran FINDSITE^{comb} (Zhou and Skolnick, 2013) to annotate computationally ligand-binding sites and EFICAZ (Kumar and Skolnick, 2012) to predict FDRs for predicted enzymes. Calculations of the free energy differences, $\Delta\Delta G$, of Trp mutations were conducted using the program DMutant, which is based on statistical potentials (Zhou and Zhou, 2002) and ranked among the top performers in an independent assessment (Khan and Vihinen, 2010). Secondary structure analysis was carried out using DSSP (Kabsch and Sander, 1983).

Statistical Analysis

With a few noted exceptions, a Fisher's exact test was conducted on the contingency table given in Table 3. A positive case is a variant containing a certain feature, such as ligand binding, or a mutation from a Cys residue. A negative case is a variant without such a feature. Outcomes are either disease associated or neutral. The counts of positive/negative cases with disease are denoted as d_{pos}/d_{neg} , respectively, and similarly, n_{pos}/n_{neg} , for positive/negative cases for neutral ones. Odds are calculated for positive and negative cases separately, and their ratio yields the OR.

Availability

The datasets are available as Supplemental Information and also online at <http://cssb.biology.gatech.edu/nssnp>.

SUPPLEMENTAL INFORMATION

Supplemental Information includes a Supplemental Spreadsheet and can be found with this article online at <http://dx.doi.org/10.1016/j.str.2015.03.028>.

ACKNOWLEDGMENTS

This work is supported by grant no. GM-37408 of the Division of General Medical Sciences of the NIH.

Received: January 26, 2015

Revised: March 3, 2015

Accepted: March 6, 2015

Published: May 28, 2015

REFERENCES

- Abecasis, G.R., Altshuler, D., Auton, A., Brooks, L.D., Durbin, R.M., Gibbs, R.A., Hurles, M.E., and McVean, G.A. (2010). A map of human genome variation from population-scale sequencing. *Nature* **467**, 1061–1073.
- Abecasis, G.R., Auton, A., Brooks, L.D., DePristo, M.A., Durbin, R.M., Handsaker, R.E., Kang, H.M., Marth, G.T., and McVean, G.A. (2012). An integrated map of genetic variation from 1,092 human genomes. *Nature* **491**, 56–65.
- Adzhubei, I., Schmidt, S., Peshkin, L., Ramensky, V., Gerasimova, A., Bork, P., Kondrashov, A., and Sunyaev, S. (2010). A method and server for predicting damaging missense mutations. *Nat. Methods* **7**, 248–249.
- Berman, H.M., Westbrook, J., Feng, Z., Gilliland, G., Bhat, T.N., Weissig, H., Shindyalov, I.N., and Bourne, P.E. (2000). The Protein Data Bank. *Nucleic Acids Res.* **28**, 235–242.
- Collins, F.S., Lander, E.S., Rogers, J., and Waterston, R.H.; International Human Genome Sequencing Consortium (2004). Finishing the euchromatic sequence of the human genome. *Nature* **431**, 931–945.
- Cooper, D.N., and Youssoufian, H. (1988). The CpG dinucleotide and human genetic disease. *Hum. Genet.* **78**, 151–155.
- de Beer, T.A., Laskowski, R.A., Parks, S.L., Sipos, B., Goldman, N., and Thornton, J.M. (2013). Amino acid changes in disease-associated variants differ radically from variants observed in the 1000 genomes project dataset. *PLoS Comput. Biol.* **9**, e1003382.
- Gao, M., and Skolnick, J. (2012). The distribution of ligand-binding pockets around protein-protein interfaces suggests a general mechanism for pocket formation. *Proc. Natl. Acad. Sci. USA* **109**, 3784–3789.
- Hubbard, S.J., and Thornton, J.M. (1993). NACCESS, Computer Program, Department of Biochemistry and Molecular Biology (University College London).
- Kabsch, W., and Sander, C. (1983). Dictionary of protein secondary structure-pattern recognition of hydrogen-bonded and geometrical features. *Biopolymers* **22**, 2577–2637.
- Khan, S., and Vihinen, M. (2010). Performance of protein stability predictors. *Hum. Mutat.* **31**, 675–684.
- Kumar, N., and Skolnick, J. (2012). EFICAZ^{2.5}: application of a high-precision enzyme function predictor to 396 proteomes. *Bioinformatics* **28**, 2687–2688.
- Kumar, P., Henikoff, S., and Ng, P. (2009). Predicting the effects of coding non-synonymous variants on protein function using the SIFT algorithm. *Nat. Protoc.* **4**, 1073–1081.
- Lee, H.J., Wang, M., Paschke, R., Nandy, A., Ghisla, S., and Kim, J.J. (1996). Crystal structures of the wild type and the Glu376Gly/Thr255Glu mutant of human medium-chain acyl-CoA dehydrogenase: influence of the location of the catalytic base on substrate specificity. *Biochemistry* **35**, 12412–12420.
- McKusick, V.A. (2007). Mendelian Inheritance in Man and its online version, OMIM. *Am. J. Hum. Genet.* **80**, 588–604.
- Metzker, M.L. (2010). Sequencing technologies—the next generation. *Nat. Rev. Genet.* **11**, 31–46.
- Ng, P.C., and Henikoff, S. (2006). Predicting the effects of amino acid substitutions on protein function. *Annu. Rev. Genomics Hum. Genet.* **7**, 61–80.
- Sobolev, V., Sorokine, A., Prilusky, J., Abola, E.E., and Edelman, M. (1999). Automated analysis of interatomic contacts in proteins. *Bioinformatics* **15**, 327–332.
- Stenson, P.D., Ball, E., Howells, K., Phillips, A., Mort, M., and Cooper, D.N. (2008). Human Gene Mutation Database: towards a comprehensive central mutation database. *J. Med. Genet.* **45**, 124–126.
- Steward, R.E., MacArthur, M.W., Laskowski, R.A., and Thornton, J.M. (2003). Molecular basis of inherited diseases: a structural perspective. *Trends Genet.* **19**, 505–513.
- Sunyaev, S., Ramensky, V., and Bork, P. (2000). Towards a structural basis of human non-synonymous single nucleotide polymorphisms. *Trends Genet.* **16**, 198–200.
- Vetel, S., Gasper, R., Eisenacher, E., and Wittinghofer, A. (2008). The retinitis pigmentosa 2 gene product is a GTPase-activating protein for Arf-like 3. *Nat. Struct. Mol. Biol.* **15**, 373–380.
- Vitkup, D., Sander, C., and Church, G.M. (2003). The amino-acid mutational spectrum of human genetic disease. *Genome Biol.* **4**, R72.
- Wang, Z., and Moulton, J. (2001). SNPs, protein structure, and disease. *Hum. Mutat.* **17**, 263–270.
- Wu, C.H., Apweiler, R., Bairoch, A., Natale, D.A., Barker, W.C., Boeckmann, B., Ferro, S., Gasteiger, E., Huang, H.Z., Lopez, R., et al. (2006). The Universal Protein Resource (UniProt): an expanding universe of protein information. *Nucleic Acids Res.* **34**, D187–D191.
- Zhou, H.Y., and Zhou, Y.Q. (2002). Distance-scaled, finite ideal-gas reference state improves structure-derived potentials of mean force for structure selection and stability prediction. *Protein Sci.* **11**, 2714–2726.
- Zhou, H., and Skolnick, J. (2013). FINDSITE^{comb}: a threading/structure-based, proteomic-scale virtual ligand screening approach. *J. Chem. Inf. Model.* **53**, 230–240.